Simulation of liquid cargo – vehicle interaction under lateral and longitudinal accelerations

†José A. Romero[1], Frank Otremba[2], and Alejandro A. Lozano Guzmán[3]

[1]Faculty of Engineering, Queretaro Autonomous University, Mexico.
[2]Federal Institute of Materials Research and Testing (BAM), Berlin.
[3]Applied Science and Advanced Technology (CICATA), Queretaro, Mexico.
†Presenting and corresponding author: jaromero@uaq.mx

Abstract

Amongst the vehicle parameters influencing road safety, the carried cargo plays a critical role in the case of a liquid cargo, posing rollover risk and affecting the available friction forces for braking. While the lateral sloshing of the cargo within the vehicle´s compartments, can be excited when the vehicle negotiates a turn, the longitudinal motion of the cargo derives from changes of speed. The combination of both types of perturbations occurs when the vehicle brakes while negotiating a turn. In this paper, a two-pendulum formulation is used to simulate the lateral and longitudinal behavior of a vehicle when negotiating a braking in a turn maneuver. The suspension forces are thus calculated as the linear superposition of both models. Results suggest that the vehicle roll stability is affected by the cargo sloshing, with increments on the order of 100% in the lateral load transfer, for a 50% filled tank. On the other hand, the dispersion of the travelling speed also affects the lateral stability of such type of vehicles, as a function of the dispersion of the vehicle´s travelling speed.

Keywords: **Sloshing cargo, road tankers, pendulum analogy, braking in a turn, lateral load transfer ratio**

Introduction

Causality for a road crash derives from an unfortunate combination of events, that potentially involves the vehicle, the driver, the infrastructure and the environment. For a road crash, different levels of contributing factors and situations are identified, including a critical event, a critical reason and a critical source [1]. While the human factors are recognized as the main contributing factors for road crashes, the factors associated to the vehicle represent a major road crashes contribution. Within the vehicle, however, different influencing elements can be identified, including the failure of the mechanical parts of the vehicle, and the condition of the cargo. The cargo contributes to road crashes in different ways, as its configuration and nature can affect the performance of the vehicle, in different ways. While the cargo configuration refers to the dimensions of the cargo or its container; its nature refers to its physical state (liquid, solid) as well its level of hazardousness. While the height of the center of gravity position of a solid cargo can affect the lateral stability of a vehicle, the shifting of such center of gravity, which is an intrinsic characteristic of a liquid cargo, can pose a major risk to vehicle´s lateral stability and longitudinal behavior. The mobility of the cargo within the carrying vehicle produces two main effects. On the one hand, the shifting of the center of gravity of the cargo, whether laterally or longitudinally, affects the balance of forces on the different ends of the vehicle, further affecting the rollover trend and the available braking force. The other potential effect of a liquid, sloshing, cargo, derives from the vibration frequency the liquid cargo. That is, the mobility of the cargo generates a coupled dynamic system with the mass-spring system, represented by the sprung and un-sprung masses of the vehicle.

The behavior of a partially filled road tanker while performing steering and braking maneuvers has been studied under the principles of several mathematical approaches, including computer fluid dynamics formulations (CFD), and some mechanical analogous formulations. Such models have been dynamic or quasi-static. Kolei et al. [2], consider the linear slosh theory for developing a hybrid multimodal and boundary-element model, to simulate the natural sloshing modes of the fluid within the tank. It is reported that the natural modes of vibration of the liquid inside the tank, can be excited as a function of the perturbation input, whether it is roll- or pitch- related. The authors assess the accuracy and computer effort to simulate the free response of the liquid inside the tank, when subjected simultaneously to longitudinal and lateral accelerations. However, the simulated tank is not suspended, that is, the contributing factors associated to the vibration of the tanker chassis, are not taken into account. Dasgupta [3], reports that the superposition of longitudinal and lateral accelerations strongly affects the longitudinal load shift, but that such superposition reduces the lateral load shift because of the cornering of the fluid within the tank. In the case of straight braking, the use of mechanical analogous models has been reported in [4] of partially filled road tankers, with high levels of validation.

In this paper, several formulations are set together to simulate the suspension forces of a 4-wheel straight road tanker carrying a liquid cargo at a partial fill level. The different models include a simplified analogous model to simulate the sprung tank containing a liquid cargo at a partial fill level, for both the roll plane and the pitch plane.

Model description

A multi-body formulation is proposed for the simulation of the response of a road tanker to perturbations derived from simultaneously changing both, direction and speed. Two similar un-coupled pendulum models are used to simulate the response of the vehicle in the roll and pitch planes. The model considers only the vibration of the sprung mass of the vehicle. That is, the effect of the un-sprung dynamics is not consider, and the flexibility provided by the tires stiffness, is assumed to be included in the equivalent torsional stiffness of the sprung mass [5].

Part (a) of Figure 1 illustrates a schematic representation of the two-axle straight road tanker, and parts (b) and (c) of this figure describe the analogous pendulum models representing the roll and pitch – plane vibration modes of the road tanker, respectively. As it can be seen in this figure, the individual suspension stiffness at the end of each vibration plane, was substituted by an equivalent torsional stiffness, producing a two-degree of freedom system, involving a simple pendulum and an inverted pendulum. A cylindrical shape for the tank is assumed in this paper. According to this model, a simple pendulum represents the sloshing cargo, while the chassis vibration is characterized in terms of an inverted pendulum.

In these models, the length of the simple pendulum is calculated in terms of a validated methodology to determine the natural sloshing frequency of the liquid inside the tank. Tue suspension springs and dampers of the 4-wheel road tanker, are assumed as having a linear behavior.

The equations of motion for the resultant mechanical system described in parts (b) and (c) of Figure 1, are derived from an Isaac Newton´s approach.

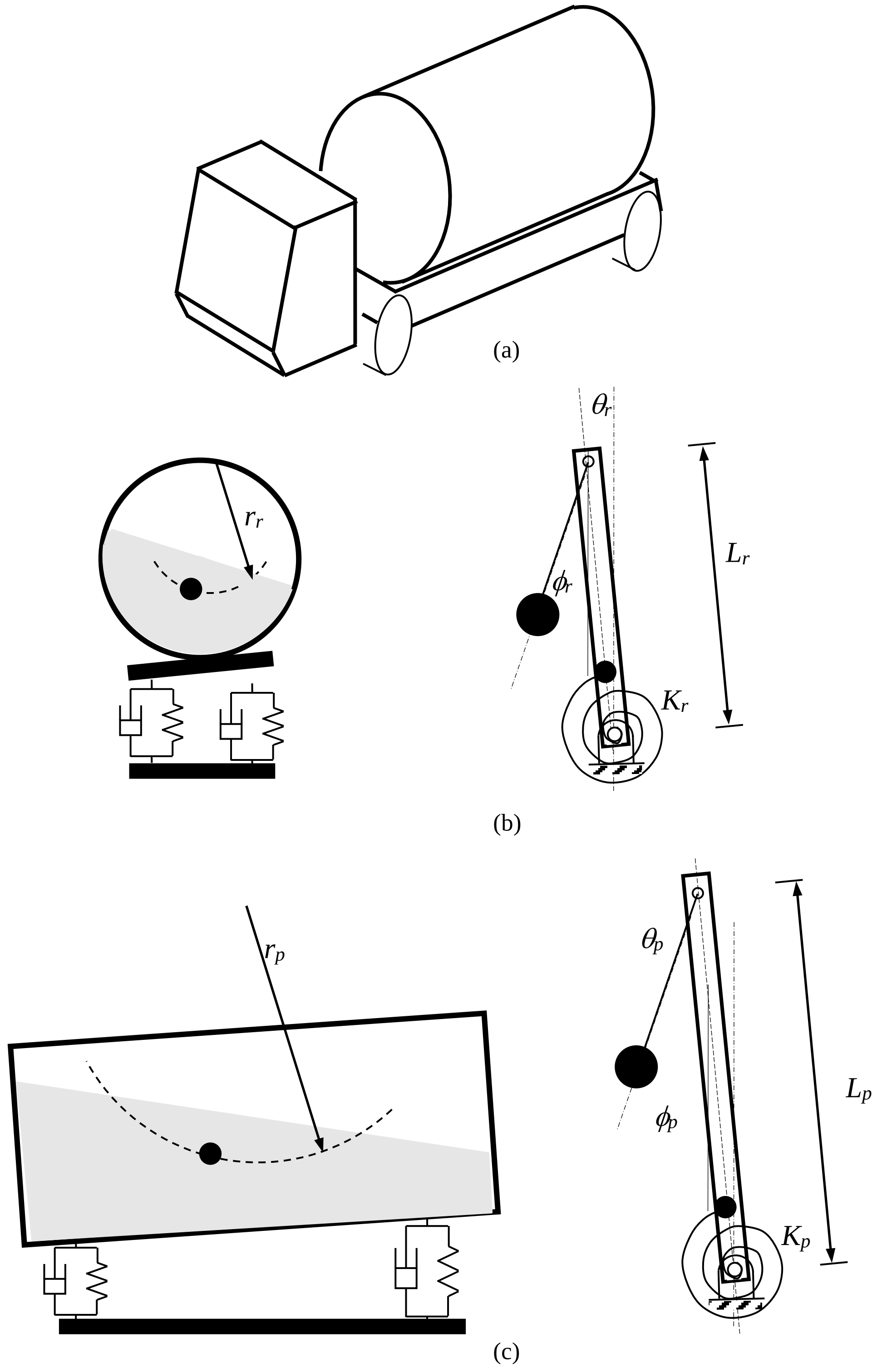

Figure 1. (a) Schematic representation of the vehicle; (b) roll vibration model; (c) pitch vibration model.

For the simple pendulum, its mass is subjected to lateral accelerations, as a result of the string tangential acceleration ($r_p \ddot{\phi}$), the inverted pendulum centripetal acceleration $L\left(\dot{\theta}\right)^2(\phi+\theta)$; and the tangential acceleration of the inverted pendulum $\ddot{\theta} L\cos(\theta)$. In this regard, the oscillation angles are considered small enough, to consider that $\sin(\phi+\theta)=\phi+\theta$; and $L\cos(\theta)=L$. The development of the equations of motion for the simple pendulum, is presented in Figure 2, and in Figure 3 the derivation of the equation of motion of the inverted pendulum, is presented. The tension of the simple pendulum that represents the sloshing cargo, is exerted on the inverted pendulum modeling the vehicle chassis. It should be noted that the center of rotation for the pendulum, is obtained from the summation of the center of gravity position of the sloshing cargo, and the length of the simple pendulum representing such cargo, r_p, whose length derivation is presented below in this paper.

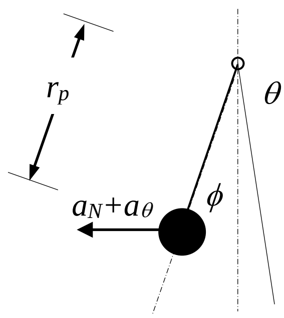

$$a_\theta = r_p \ddot{\phi} - L\left(\dot{\theta}\right)^2(\phi+\theta) + \ddot{\theta} L\cos(\theta) \tag{1}$$

$$-mg\phi = ma_\theta = m\left[r_p \ddot{\phi} - L\left(\dot{\theta}\right)^2(\phi+\theta) + \ddot{\theta} L\cos(\theta)\right]$$

$$-mg\phi = ma_\theta = m\left[r_p \ddot{\phi} - L\left(\dot{\theta}\right)^2(\phi+\theta) + \ddot{\theta} L\cos(\theta)\right]$$

$$\ddot{\phi} = \phi\left[-\frac{g}{r_p} + \frac{L}{r_p}\left(\dot{\theta}\right)^2\right] + \frac{L}{r_p}\left(\dot{\theta}\right)^2\theta - \frac{\ddot{\theta}}{r_p} L\cos(\theta)$$

Figure 2. Equations of motion derivation for the simple pendulum representing the sloshing cargo (similar models for pitch and roll vibration)

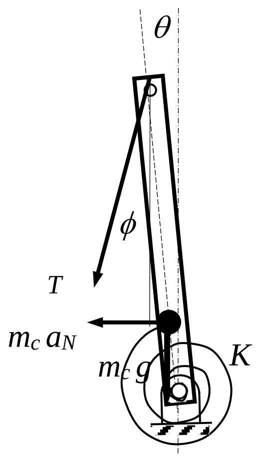

$$\ddot{\theta} = \frac{1}{I_p}\left\{-K\theta - C\dot{\theta} + T\left(\cos(\phi)L\theta + \sin(\phi)L\cos(\theta)\right)\right\} \tag{2}$$

where:

$$T = mg\cos(\phi) + ma_r$$

where:

$$a_r = \ddot{\theta} L\cos[(\pi/2) - \phi - \theta] + L\left(\dot{\theta}\right)^2\cos(\phi+\theta) - L\left(\dot{\theta}\right)^2$$

Figure 3. Equations of motion derivation for the inverted pendulum representing the vehicle chassis cargo (similar models for pitch and roll vibration)

The coupled equations of motion (1) and (2) are solved through the Transition Matrix Methodology (TMM), which represents a computationally efficient method for obtaining the dynamic response of linear mechanical systems in the time dominium. In this regard, some variables in Eq. (1) are also the outputs from the model, so that the time response will be obtained on the basis of previous outputs from the model.

According to the TMM scheme, the coupled equations of motion (1) and (2) are expressed as a first order system, on the basis of State Vector variables, as follows:

$$\left\{\dot{y}(t)\right\} = [A]\{y(t)\} + [B]_1\{Y_1(t)\} + [B]_2\{Y_2(t)\} \tag{3}$$

where: $\left\{\dot{y}(t)\right\} = \left\{\dot{\phi} \quad \ddot{\phi} \quad \dot{\theta} \quad \ddot{\theta}\right\}^T$; $\{Y_1(t)\} = \left\{0 \quad \ddot{\theta} \quad 0 \quad \ddot{\phi}\right\}^T$; $\{Y_2(t)\} = \{0 \quad a_N \quad 0 \quad 0\}^T$

$$[A] = \begin{bmatrix} 0 & 1 & 0 & 0 \\ -\dfrac{9.81}{r_p} & -\dfrac{C_A}{m} & -\dfrac{L_B\left(\dot{\theta}\right)^2}{r_p} & 0 \\ 0 & 0 & 0 & 1 \\ \dfrac{T\phi\, L_B \cos\theta}{I_p} & 0 & \dfrac{T\phi\, L_B \cos\theta - K_\theta}{I_p} & -\dfrac{C_\theta}{I_p} \end{bmatrix}$$

$$[B]_1 = \begin{bmatrix} 0 & 0 & 0 & 0 \\ 0 & -\dfrac{L_B}{r_p}\cos\theta & 0 & 0 \\ 0 & 0 & 0 & 0 \\ 0 & 0 & 0 & 0 \end{bmatrix} \qquad [B]_2 = \begin{bmatrix} 0 & 0 & 0 & 0 \\ 0 & -\dfrac{1}{r_p}0 & 0 & 0 \\ 0 & 0 & 0 & 0 \\ 0 & \dfrac{m\, w\, L_B}{I_p} & 0 & \dfrac{1}{I_p} \end{bmatrix}$$

The solution of Equation (3), proceeds according to the Transition Matrix Approach [6], where the discrete time response is expressed as follows:

$$\{y(t+\Delta t)\} = [\Phi]\{y(t)\} + [\Gamma]_1\{Y_1(t)\} + [\Gamma]_2\{Y_2(t)\} \tag{4}$$

where: $[\Phi] = e^{[A]\Delta t} = [1] + \Delta t[A] + \dfrac{\Delta t^2}{2!}[A]^2 + \dfrac{\Delta t^3}{3!}[A]^3 + \ldots\ldots\ldots\ldots \dfrac{\Delta t^n}{n!}[A]^n$

and: $\Gamma_1 = [A]^{-1}(\Phi - I)[B_1]; \quad \Gamma_2 = [A]^{-1}(\Phi - I)[B_2]$

On the other hand, when incorporating into a curve that has a constant radio, the vehicle is subjected to transient accelerations before it is subject to the acceleration derived from the constant radius turn. The transition from an infinite, straight road segment, into a constant radius turn, represents different transition radiuses, as it is illustrated in Figure 4, where the representation is simplified into a bicycle model. The details of the model are presented in [7].

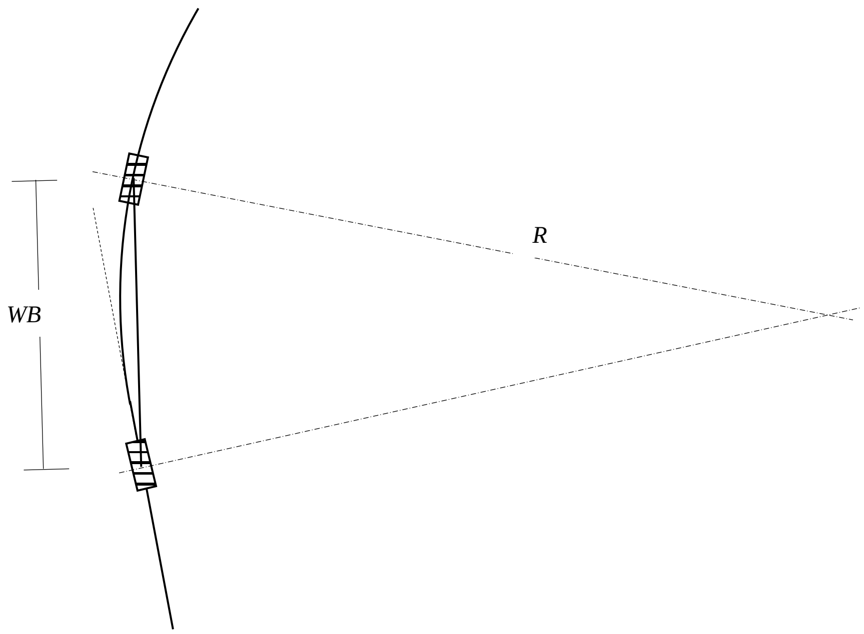

Figure 4. Transition from a straight into a constant radius curve.

The pendulum length r_p in the above equations, is calculated on the basis of a validated methodology reported in [8], based upon the sloshing motion in a rectangular tank of length L as follows:

$$2Lf = \left(\frac{g}{\kappa} \tanh \kappa H \right)^{1/2} \tag{5}$$

where H is the depth of the rectangular tank, L is the free length of the fluid surface, and κ is the wave number = $2\pi / \lambda$, where $\lambda = 2L$ This formula has been successfully used for non-rectangular tank situations, if an equivalent depth H_e is used, as a function of the cross sectional area of the tank, as follows [9]:

$$H_e = \frac{Area}{L_f} \tag{6}$$

where L_f is the length of the free surface.

Results

The described model is used to simulate the behavior of a half-filled road tanker under two circumstances: when making a brake in a turn maneuver, and when travelling along a winding road. For the braking in a turn maneuver, two different turn radiuses are considered, for an initial vehicle speed (30 km/h). Table 1 lists the values for the different vehicle properties, including the lengths of the pendulums for the roll and pitch modes of vibration. For half-filled circular tank, the center of gravity, is located at 0.5 m from the free surface. For the calculation of the natural frequency, a tank diameter is considered of 2.4 m, while the length is determined as 6.6 m for a 30 cubic meters capacity straight road tanker. The corresponding natural sloshing frequencies for the roll and pitch sloshing, according to the formulation described above, are 0.52 Hz and 0.24 Hz, respectively, resulting in pendulum lengths of 0.9 m, and 4.06 m, respectively,

Table 1. Properties of the vehicle

Equivalent torsional stiffness (pitch)	118300000 N-m/rad
Equivalent torsional stiffness (roll)	7056000 Nm/rad
Simple pendulum length (pitch)	4.06 m
Simple pendulum length (roll)	0.9 m
Chassis mass moment of inertia (pitch)	652 km-m^2
Chassis mass moment of inertia (roll)	1305 km-m^2
Chassis mass	4000 kg
Liquid mass	15000 kg
Working fluid	Water
Vehicle wheelbase	6.5 m

Performance measure

The load transfer that affects the vehicle when performing a braking in a turn maneuver, is characterized in terms of the lateral load transfer ratio (*LLTR*), as follows:

$$LLTR = \mathrm{abs}(F_L - F_R) / (F_L + F_R) \tag{7}$$

where F_L is the suspension force on the left side, and F_R is the right suspension force. According to this expression, *LLTR* can have a value from 0 to 1, where 1 means that one side of the vehicle is losing contact with the road. While the standard *LLTR* is calculated based on the tire forces, in this paper such forces are the suspension forces. Furthermore, in the case of the three-dimensional situation considered in this paper, two *LLTR* shall be calculated, on the front and rear sides.

Braking in a turn maneuver

Figures 5 and 6 illustrate the simulation results when the vehicle performs an emergency braking in a turn maneuver at 3.5 m/s^2, for an initial speed of 30 km/h. Parts (a) and (c) of these figures describe the time history of the four suspension forces involved: front and rear; left and right. While part (a) corresponds to a braking maneuver on a 500-meter radio curve, part (c) describes the results for a tighter turning maneuver, corresponding to a 287 m curve. Parts (b) and (d) describe the corresponding values of the *LLTR*, for the front and rear suspension positions. According to these results, reducing from 500-meter to 287 meters the radius of the turn (42% reduction), causes an increase in the maximum *LLTR* from 0.4 to 0.7 (75%). Consequently, the is a non-linear effect of the turning radius on the rollover trend of the vehicle. In can also be noted that, regardless of the turning radius involved, the maximum value for *LLTR* occurs after about 5 cycles of chassis – liquid cargo interaction. Additionally, it can be observed that the greater rollover trend occurs in the case of the front axle.
Figure 7 describes a summary of the effect of both cargo condition and curve radius, on the maximum values obtained for the *LLTR*.

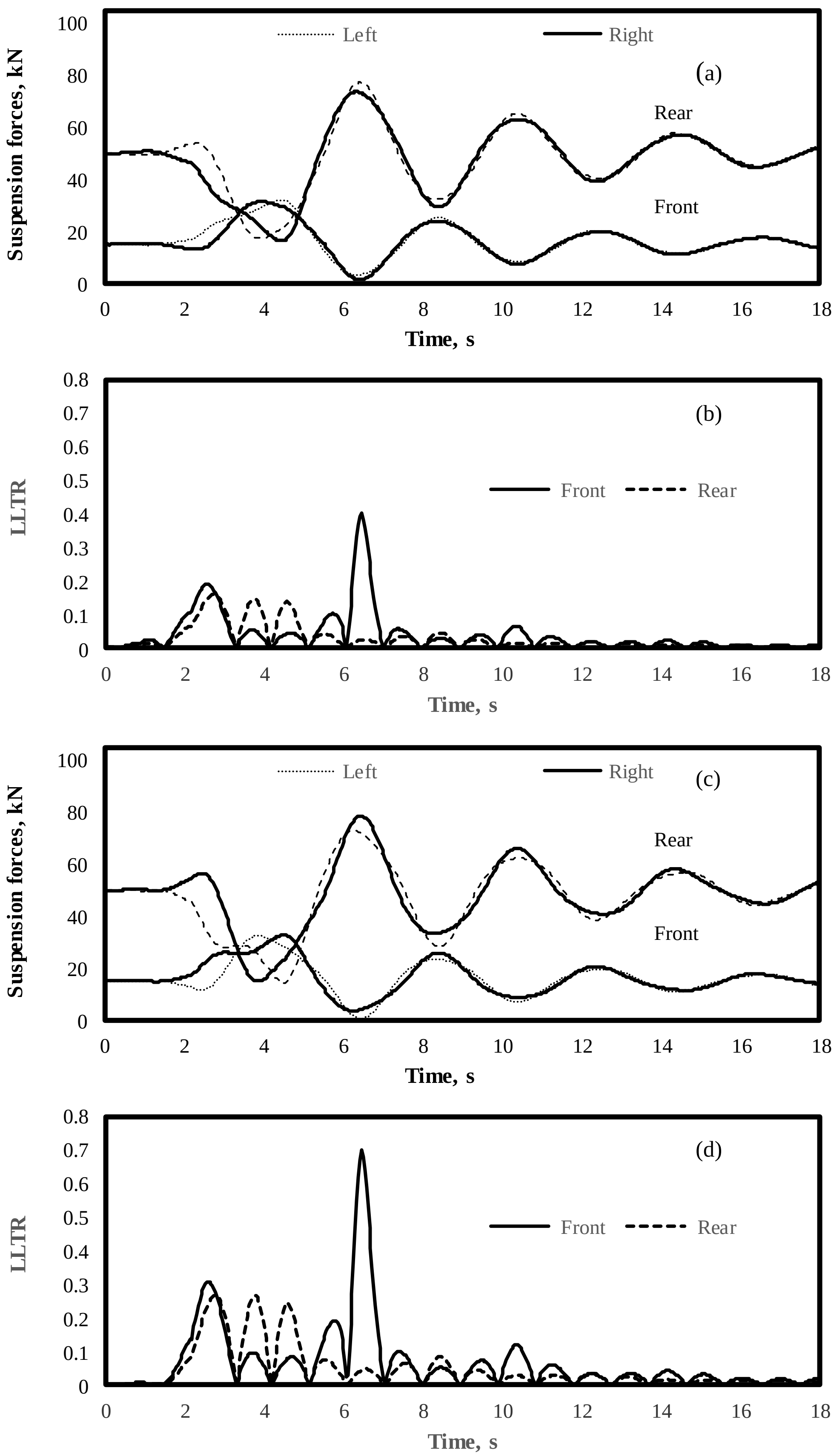

Figure 5. Braking in a turn, two different radiuses, from 30 km/h: (a) and (b) 500 m radius curve; (c) and (d) 325 m radius curve (Sloshing cargo)

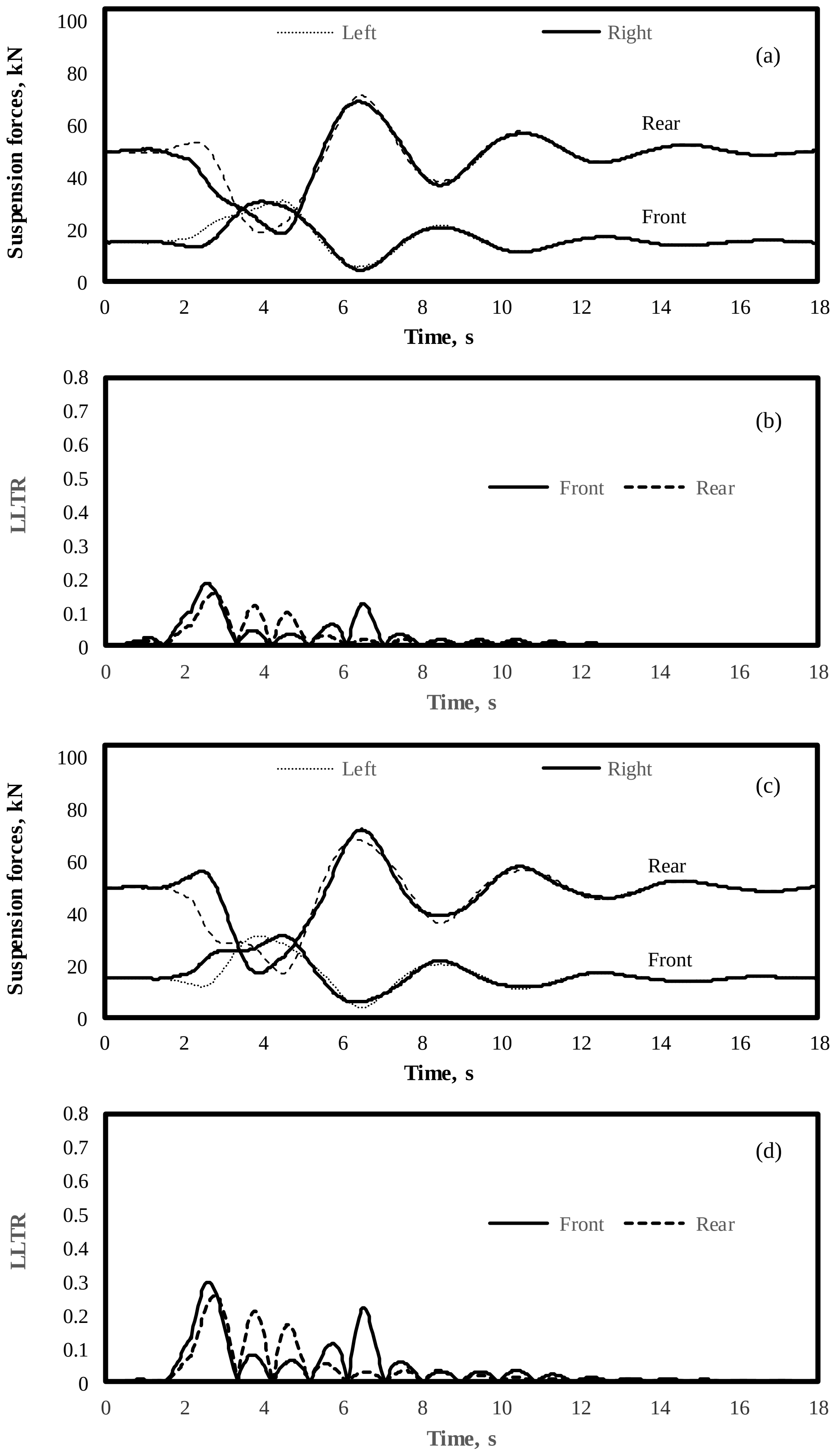

Figure 6. Braking in a turn, several radiuses, from 30 km/h: (a) and (b) 500 m radius curve; (c) and (d) 325 m radius curve (Non-sloshing cargo)

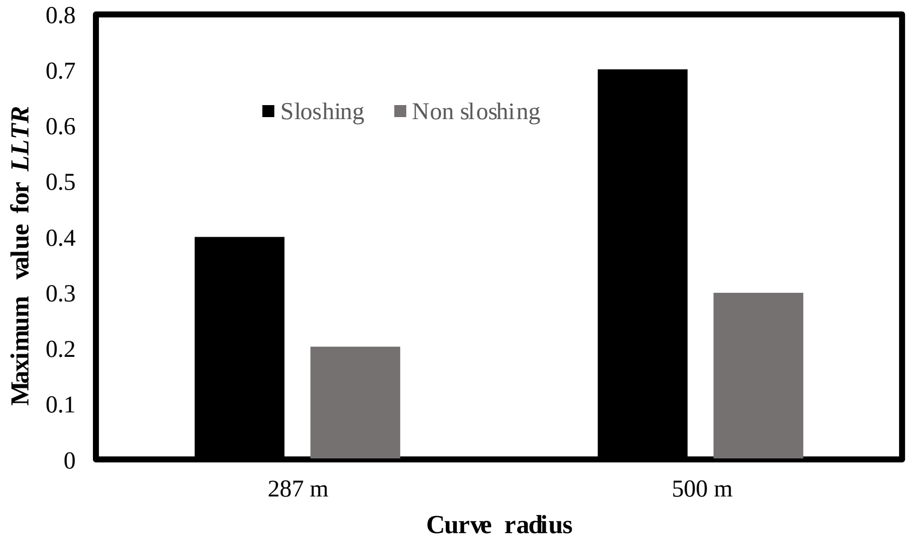

Figure 7. Load transfers during braking in a turn maneuver, for two curve radiuses and cargo condition.

Winding road

The journey of the road tanker along a 4-curve road is now presented. Figure 8 describes the road geometry, involving the merging of actual road curves in a 70 second journey involving a 583 m length road, where the second and third curves have different directions. The formulation described above was used to calculate the instantaneous curving radius for the transition from straight to the constant radius curve. A sample of the instantaneous turning radius is presented in Figure 9, where the maximum values are assumed as straight segments. To assess the effect of the driving style on the lateral stability of the vehicle, two levels of dispersion for the driving speed, are presented. Figures 10 to 12 illustrate the input and performance results for three levels of speed dispersion: great (dispersed), medium and zero. The coefficient of variation (COV) of the rough dispersed speed input, is 12.49%, while the corresponding value for the medium dispersed speed, is 5%.

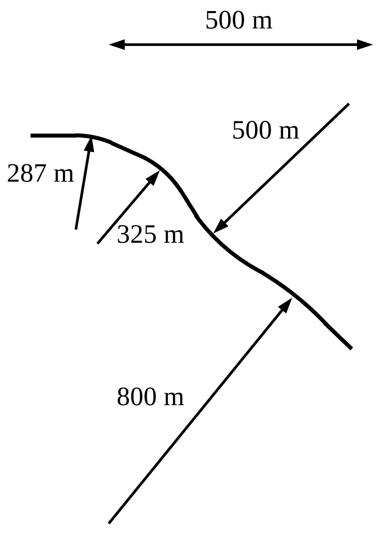

Figure 8. Road geometry for assessing roll stability of a partially filled straight road tanker

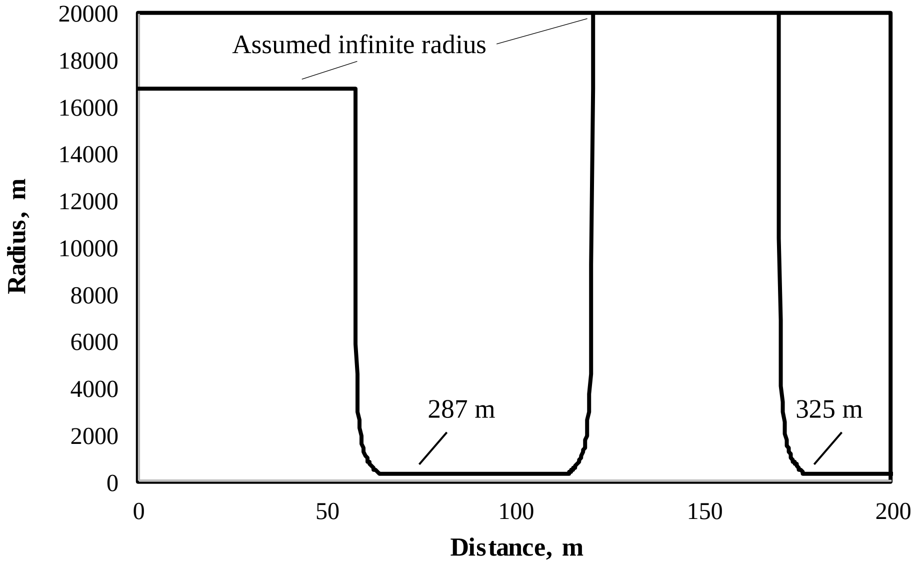

Figure 9. Sample transitional radius for the 287-m and 325-m turns.

According to these results, the dispersion in speed has a significant effect on the lateral stability of the vehicle, as an increase from the medium to the greater dispersion (150% increase) represents an increase in the maximum lateral load transfer from 0.59 to 0.88, that is, an increase of 151%. While this is a linear relationship, it should be noted that the peaks in the *LLTR*, occur in very different positions along the road. On the other hand, eliminating any dispersion of the speed, involves a reduction in the maximum *LLTR* (0.4). Figure 13 illustrates the effect of speed dispersion (COV) on *LLTR*` average value. According to these results, increasing from zero to a medium speed dispersion, involves only a small effect on the average *LLTR*, while changing from medium to rough speed dispersion, involves a significant increase of the average *LLTR*.

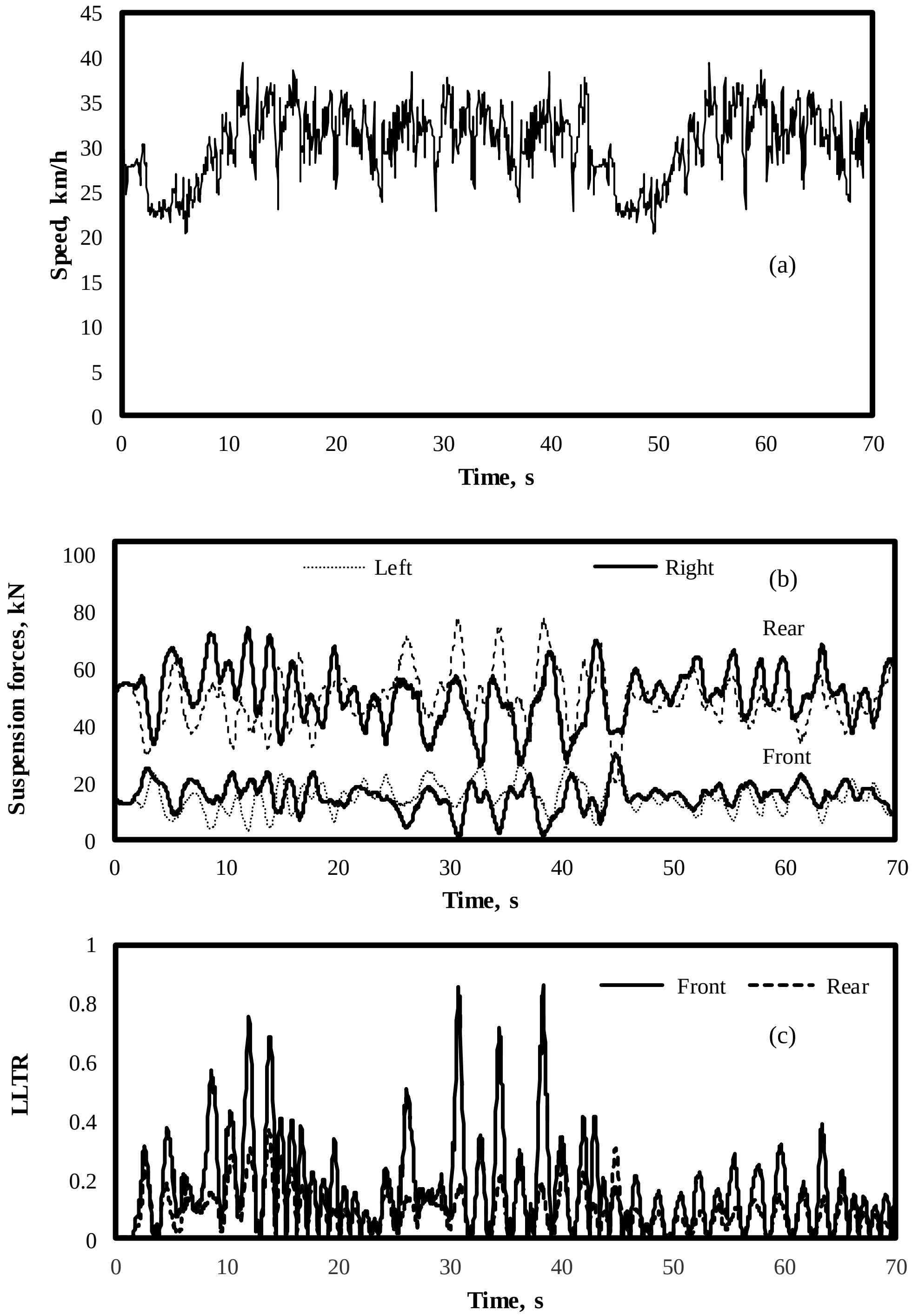

Figure 10. Performance measures for the road tanker on the winding road of Fig. 7, for a disperse speed situation

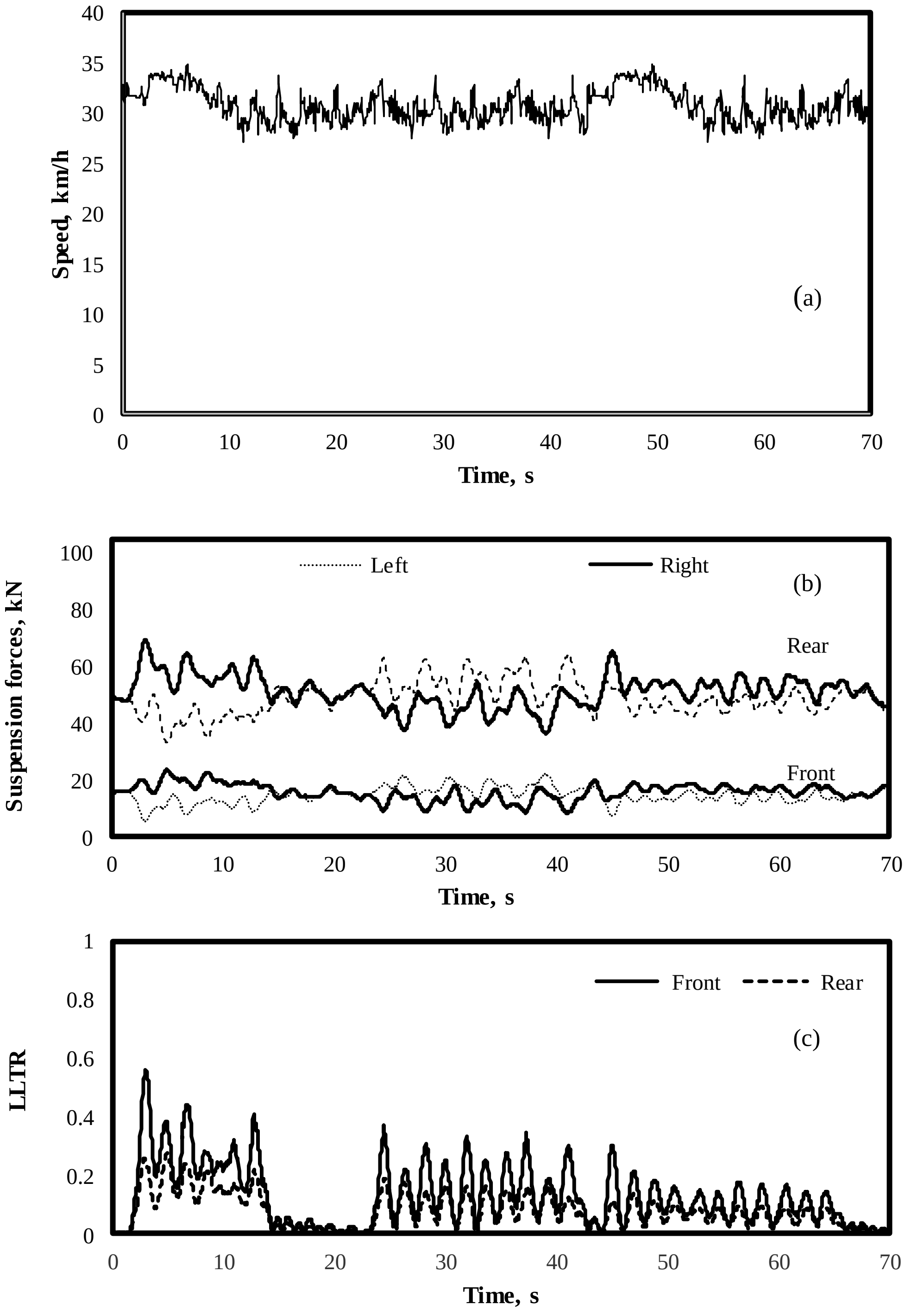

Figure 11. Performance measures for the road tanker on the winding road of Fig. 7, for a medium speed dispersion situation

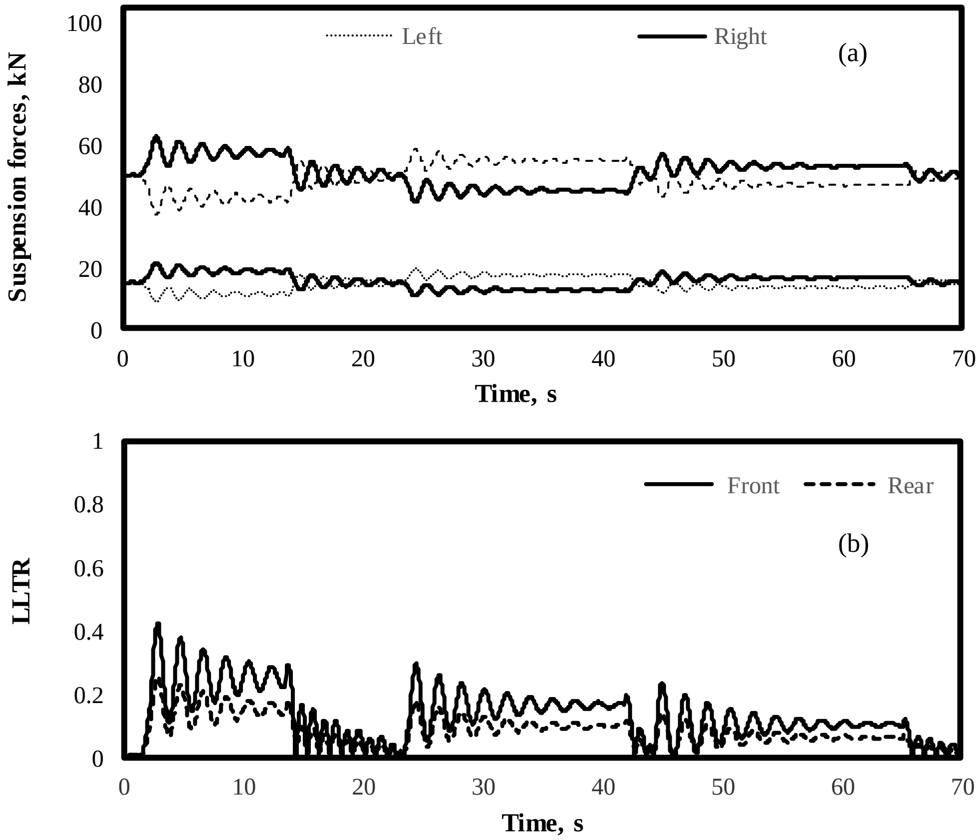

Figure 12. Performance measures for the road tanker on the winding road of Fig. 7, for a constant speed situation (30.64 km/h)

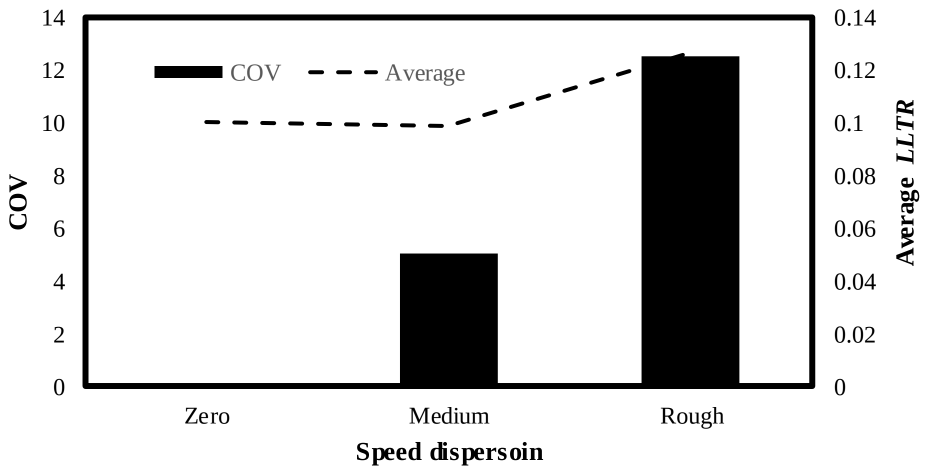

Figure 13. Effect of speed dispersion on COV and average *LLTR*

Conclusions

A simplified model is being proposed to simulate a braking in a turn maneuver of a straight road tanker. The model involves two uncoupled sets of inverted and simple pendulum models, representing the sprung mass and the sloshing cargo in the vehicle, respectively, for the longitudinal and lateral planes. Several formulations are assembled for this purpose, including the dimensioning of the simple pendulum on the basis of a validated methodology, and the transient radius when the vehicle transits from a straight to a constant radius curve. The results illustrate the longitudinal and lateral load transfer due to the braking in a turn maneuver, suggesting a nonlinear relationship between the magnitude of the radius and the maximum value reached for the selected performance measure (lateral load transfer ratio). On the other hand, the dispersion in the travelling speed also represents significant variations in the vehicle performance, when it runs along a winding road. While the main simplification of the composed model consists of the uncoupling between the longitudinal and the lateral response models, the overall response obtained is congruent with what has been reported in the literature, about the risk associated to braking while turning. Some validation elements should be provided as a continuation this research effort.

References

[1] NHTSA (2015) Critical reasons for crashes investigated in the National Motor Vehicle Crash Causation Survey. National Highway Traffic Safety Administration. DOT HS 812 115.

[2] Kolei, A., Rakheja, S., and Richard, R. (2015) Three-dimensional dynamic liquid slosh in partially-filled horizontal tanks subject to simultaneous longitudinal and lateral excitations.

[3] Dasgupta, A. (2011) Effect of tank cross section and longitudinal baffles on transient liquid slosh in partly-filled road tankers. Master of Science Thesis. Concordia University, Montreal.

[4] Romero, J.A., and Otremba, F. (2016) Experimental and theoretical modeling of cargo sloshing during braking. IMECE2016-65698.

[5] Romero, J.A., Hildebrand, R., Ortiz, W., and Gomez, J.C. (2005) Study of roll motions in high-filled tank trucks using minimum instrumentation. SAE paper 2005-01-2264.

[6] Meirovitch, L. (1986) Elements of vibration analysis. Mc Graw Hill Int. 2nd ed. 345 pp.

[7] Romero, J.A., Lozano-Guzmán, A.A., and Arroyo-Contreras, G.M. (2015) Proceedings, 2015 IFToMM World Congress. Taipei, Taiwan.

[8] Elmore, C.W. and Heald, M.A. (1989) Physics of waves, Dover Publications Inc. New York.

[9] Romero, J.A., Hildebrand, R., Ortiz, W., and Gomez, J.C. (2005B) Natural sloshing frequencies of liquid cargo road tankers, International Journal of Heavy Vehicle Systems 12(2): 121-138.